

## Spin-Orbital Coupling in a Triplet Superconductor-Ferromagnet Junction

Paola Gentile,<sup>1,2</sup> Mario Cuoco,<sup>1,2</sup> Alfonso Romano,<sup>1,2</sup> Canio Noce,<sup>1,2</sup> Dirk Manske,<sup>3</sup> and P. M. R. Brydon<sup>4</sup>

<sup>1</sup>*SPIN-CNR, I-84084 Fisciano (Salerno), Italy*

<sup>2</sup>*Dipartimento di Fisica “E. R. Caianiello,” Università di Salerno, I-84084 Fisciano (Salerno), Italy*

<sup>3</sup>*Max-Planck-Institut für Festkörperforschung, Heisenbergstrasse 1, D-70569 Stuttgart, Germany*

<sup>4</sup>*Institut für Theoretische Physik, Technische Universität Dresden, D-01062 Dresden, Germany*

(Received 31 July 2012; revised manuscript received 24 February 2013; published 27 August 2013)

We study the interplay of spin and orbital degrees of freedom in a triplet superconductor-ferromagnet junction. Using a self-consistent spatially dependent mean-field theory, we show that increasing the angle between the ferromagnetic moment and the triplet vector order parameter enhances or suppresses the  $p$ -wave gap close to the interface, according to whether the gap antinodes are parallel or perpendicular to the boundary, respectively. The associated change in condensation energy establishes an orbitally dependent preferred orientation for the magnetization. When both gap components are present, as in a chiral superconductor, first-order transitions between different moment orientations are observed as a function of the exchange field strength.

DOI: [10.1103/PhysRevLett.111.097003](https://doi.org/10.1103/PhysRevLett.111.097003)

PACS numbers: 74.45.+c, 74.20.Rp, 74.50.+r

*Introduction.*—The singlet superconductor (SSC) and ferromagnet (FM) phases are fundamentally incompatible, as the exchange field of the FM destroys the superconductivity by aligning the antiparallel spins of the electrons in singlet Cooper pairs [1]. This pair-breaking effect makes the homogeneous coexistence of SSC and FM very rare. On the other hand, SSC-FM interfaces can be readily fabricated in artificial heterostructures, and the study of these devices has attracted intense attention [2–7]. The pair-breaking effect is central to the understanding of these systems; e.g., it causes the spatial oscillation of the SSC correlations in the barrier of a ferromagnetic Josephson junction, which is responsible for the famed  $0$ - $\pi$  transition [2,3]. The FM also suppresses the SSC gap close to the interface [2,6,7], and can induce a magnetization in the SSC [4]. Conversely, in order to minimize pair breaking in the SSC, the magnetization in the FM may be suppressed near to the interface [4], while domains may spontaneously form in a thin FM layer [5].

The coexistence of FM and triplet superconductor (TSC) states is more favorable, as the exchange field is only pair breaking when it is perpendicular to the Cooper pair spins. The physics of TSC-FM devices is therefore richer than their singlet counterparts, as the orientation of the FM moment relative to the TSC vector order parameter is now a crucial variable. This is predicted to control the nature of the proximity effect in TSC-FM bilayers [8] and the sign of the current in TSC-FM-TSC Josephson junctions [9]. In addition to the pair breaking, spin-flip reflection processes at the interface with the FM scatter the triplet Cooper pairs between the spin  $\uparrow$  and  $\downarrow$  condensates, setting up a Josephson-like coupling between them. The resulting “spin Josephson effect” is manifested as a spontaneous spin current in the TSC normal to the TSC-FM interface [10,11].

The pair breaking and spin Josephson coupling both make significant contributions to the free energy of a TSC-FM junction through the proximity effect, interface electronic reconstruction, and the variation of the TSC gap. Although these contributions depend upon the direction of the FM’s exchange field, the two effects do not necessarily act constructively: while pair breaking is always absent for a moment perpendicular to the TSC’s vector order parameter, the effective Josephson phase difference can vanish for parallel and perpendicular configurations, depending on the orbital pairing state. It is the purpose of this Letter to explore in an unbiased way the interplay of the spin and orbital structure of the TSC in setting the stable orientation of the FM’s moment. This is a timely problem, as the recent preparation [12] of superconducting thin films of  $\text{Sr}_2\text{RuO}_4$  [13] opens the way to TSC heterostructures. Furthermore, the proposed appearance of Majorana fermions at TSC-FM interfaces in quantum wires motivates a deeper understanding of the interplay between FM and TSC [14].

To this purpose we study a lattice model of a TSC-FM heterostructure using a self-consistent Bogoliubov–de Gennes theory [6,15]. For a single-component  $p$ -wave TSC, we find that the variation of the gap controls the orientation of the FM’s moment via the change in condensation energy. The stable configuration is either parallel or perpendicular to the TSC vector order parameter, depending on the alignment of the TSC gap with respect to the interface, thus evidencing a unique form of *spin-orbital coupling*. The stable configuration for the chiral  $p_x + ip_y$  state evidences competition between the different orbital components, with a first-order transition from the perpendicular to the parallel configuration as the FM exchange field is increased. When the interface is imperfect, other processes play the decisive role in setting the easy axis in the FM.

*The model.*—We examine a lattice model of the TSC-FM junction shown in Fig. 1(a). The lattice size is  $(L + 1) \times (L + 1)$ , with periodic boundary conditions imposed along the direction parallel to the interface. Indicating each site by a vector  $\mathbf{i} \equiv (i_x, i_y)$ , with  $i_x$  and  $i_y$  being integers ranging from  $-L/2$  to  $L/2$ , we write the Hamiltonian

$$H = - \sum_{\langle \mathbf{i}, \mathbf{j} \rangle, \sigma} t_{\mathbf{i}, \mathbf{j}} (c_{\mathbf{i}\sigma}^\dagger c_{\mathbf{j}\sigma} + \text{H.c.}) - \mu \sum_{\mathbf{i}, \sigma} n_{\mathbf{i}\sigma} - \sum_{\langle \mathbf{i}, \mathbf{j} \rangle \in \text{TSC}} V (n_{\mathbf{i}\uparrow} n_{\mathbf{j}\downarrow} + n_{\mathbf{i}\downarrow} n_{\mathbf{j}\uparrow}) - \sum_{\mathbf{i} \in \text{FM}} \mathbf{h} \cdot \mathbf{s}_{\mathbf{i}}, \quad (1)$$

where  $c_{\mathbf{i}\sigma}$  is the annihilation operator of an electron with spin  $\sigma$  at the site  $\mathbf{i}$ ,  $n_{\mathbf{i}\sigma} = c_{\mathbf{i}\sigma}^\dagger c_{\mathbf{i}\sigma}$  is the spin- $\sigma$  number operator, and  $\mathbf{s}_{\mathbf{i}} = \sum_{s, s'} c_{\mathbf{i}s}^\dagger \boldsymbol{\sigma}_{s, s'} c_{\mathbf{i}s'}$  is the local spin density. The lattice is divided into three regions: the FM subsystem for  $i_x < 0$ , the TSC subsystem for  $i_x > 0$ , and the interface at  $i_x = 0$ . The chemical potential  $\mu$  is the same across the lattice. The hopping matrix elements  $t_{\mathbf{i}, \mathbf{j}} = t$  everywhere, except for hopping between the ordered subsystems where  $t_{\mathbf{i}, \mathbf{j}} = t_{\text{int}} > t$  ( $< t$ ) models an imperfect interface with enhanced (suppressed) charge transfer probability. All energy scales are expressed in units of  $t$ . A nearest-neighbor attractive interaction  $-V < 0$  is present only on the TSC side of the junction. The order parameter of the TSC, the so-called  $\mathbf{d}$ -vector, encodes the spin structure of the Cooper pairs: it is defined as  $\mathbf{d} = (1/2) \times (\Delta_1 - \Delta_{-1})\hat{\mathbf{x}} - (i/2)(\Delta_1 + \Delta_{-1})\hat{\mathbf{y}} + \Delta_0\hat{\mathbf{z}}$ , where  $\Delta_{S_z}$  is the gap for triplet pairing with the  $z$  component of the spin  $S_z = -1, 0, 1$ . In our model, Eq. (1), a TSC state with the  $\mathbf{d}$ -vector parallel to the  $z$  axis can be stabilized at the mean-field level by tuning the electron density and pairing strength. We consider  $p_x$ ,  $p_y$ , and  $p_x + ip_y$  orbital symmetries for the pairing amplitude. The FM subsystem is modeled by the exchange field  $\mathbf{h}$ , which forms the angle  $\phi$  with respect to the direction of the  $\mathbf{d}$ -vector. Since the TSC state is invariant under spin rotations about the  $\mathbf{d}$ -vector,  $\mathbf{h}$  can be restricted to the  $x$ - $z$  plane, i.e.,  $\mathbf{h} = h(\sin(\phi), 0, \cos(\phi))$ . The relation between the amplitude

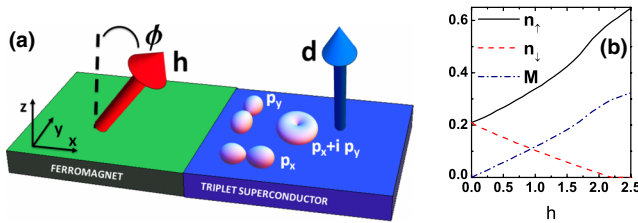


FIG. 1 (color online). (a) Schematic diagram of the two-dimensional TSC-FM junction. The FM region is located at  $x < 0$ , while the TSC is realized for  $x > 0$ . The magnetization  $\mathbf{M}$  of the FM is collinear to the exchange field  $\mathbf{h}$  and forms an angle  $\phi$  with the  $\mathbf{d}$ -vector of the TSC, which defines the  $z$  axis. We study TSC states with  $p_x$ ,  $p_y$ , and  $p_x + ip_y$  symmetry. (b) Evolution of the bulk FM magnetization and the majority and minority spin concentrations as a function of the exchange field  $h$ .

of the magnetization  $\mathbf{M}$  and  $\mathbf{h}$  is shown in Fig. 1(b), with  $\mathbf{M}$  being collinear to  $\mathbf{h}$ .

We obtain a single-particle Hamiltonian  $H_{MF}$  from Eq. (1) by decoupling the interaction term and solving self-consistently for the mean-field amplitudes  $\Delta_{\mathbf{ij}} = \langle c_{\mathbf{i}}^\dagger c_{\mathbf{j}} \rangle$ , with the average  $\langle A \rangle$  being the thermal expectation value of the operator  $A$  [16]. We hence calculate the condensation energy  $E_\Delta$  of the TSC and the Gibbs free energy  $F$  of the junction,

$$E_\Delta = \frac{V}{L^2} \sum_{\langle \mathbf{i}, \mathbf{j} \rangle \in \text{TSC}} |\Delta_{\mathbf{ij}}|^2, \quad (2)$$

$$F = - \frac{1}{L^2 \beta} \ln \{ \text{Tr} [\exp(-\beta H_{MF})] \}, \quad (3)$$

where  $\beta = (k_B T)^{-1}$  and  $k_B$  is the Boltzmann constant. The magnetization is determined by summing over the local spin density in the FM region, i.e.,  $\mathbf{M} = (4/L^2) \sum_{\mathbf{i} \in \text{FM}} \langle \mathbf{s}_{\mathbf{i}} \rangle$ . The results presented here were obtained using  $L = 120$ ; a larger lattice does not qualitatively change our conclusions.

In our analysis of the TSC-FM junction we first aim to understand how the pairing potential changes with the magnetization orientation. For this it is convenient to assume that the angle  $\phi$  is *fixed*. The observed changes in the pairing potential as a function of  $\phi$  then motivates us to treat  $\phi$  as a *variational parameter*, and to seek the most stable magnetic configuration. These individual steps have physical relevance: the former models the case where the magnetization in the FM is strongly pinned by anisotropy or an external field, whereas the latter corresponds to the limit of an isotropic FM where the TSC acts as the unique source of spin symmetry breaking.

*Pairing amplitude.*—In Fig. 2 we present the pairing amplitude profile near the interface for  $h = 1.5$ ,  $t_{\text{int}} = 1$ ,

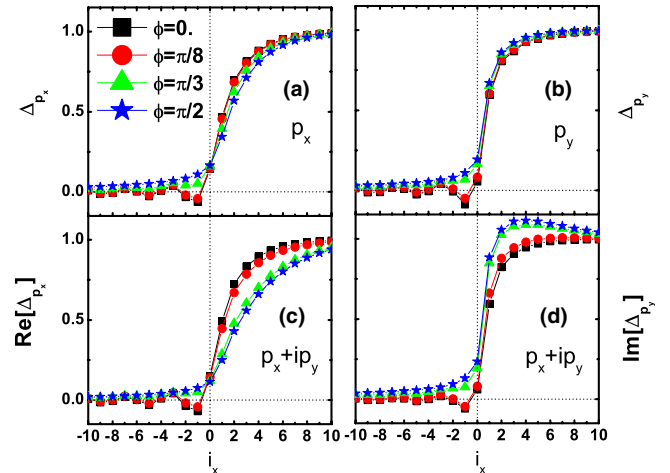


FIG. 2 (color online). Zero temperature pairing amplitude scaled to its bulk value as a function of the distance  $i_x$  from the interface for  $h = 1.5$ ,  $t_{\text{int}} = 1$ , and several different angles  $\phi$  of the  $\mathbf{d}$ - $\mathbf{M}$  misalignment. The spin-triplet orbital symmetry is of (a)  $p_x$ , (b)  $p_y$ , and chiral type with (c) a real  $p_x$  and (d) an imaginary  $p_y$  component, respectively.

and several different values of  $0 \leq \phi \leq \pi/2$ . This is determined by minimizing the Gibbs energy functional with respect to the pairing amplitudes at the fixed angle [16]. Distinct trends are evident both in the FM and TSC sides of the junction as the exchange field is rotated from a parallel ( $\phi = 0$ ) to a perpendicular ( $\phi = \pi/2$ ) orientation with respect to the  $\mathbf{d}$ -vector. Independent of the orbital symmetry, the proximity effect in the FM smoothly evolves from a monotonic decay at  $\phi = \pi/2$  to a damped oscillating behavior at  $\phi = 0$  [8]. The oscillating behavior is similar to that observed in an SSC-FM junction [2], and is also due to pair breaking, specifically the *spin-spin* coupling between the  $z$  component of the exchange field and the in-plane spin of the triplet Cooper pairs.

In contrast, the pairing amplitude in the TSC side of the interface strongly depends upon both the angle  $\phi$  and the *orbital* symmetry of the TSC. For a TSC with  $p_x$  orbital symmetry, the pairing amplitude near the interface is reduced as the exchange field is tilted from parallel to perpendicular with respect to the  $\mathbf{d}$ -vector [see Fig. 2(a)]; the opposite behavior is observed for a  $p_y$  TSC, although the effect is less pronounced [see Fig. 2(b)]. The chiral  $p_x + ip_y$  TSC evidences both trends: decreasing  $\phi$  from  $\pi/2$  to 0 enhances the real ( $p_x$ ) part of the gap [Fig. 2(c)], but suppresses the imaginary ( $p_y$ ) part [Fig. 2(d)]. Competition between the two gap components enhances their variation with  $\phi$  compared to the time-reversal symmetric states.

The pair breaking due the spin-spin coupling cannot explain the different  $\phi$  dependence of the  $p_y$  and  $p_x$  gap profiles. This instead originates from the spin-flip reflection of triplet Cooper pairs at the interface with the FM, which is crucial for the spin Josephson effect [10,11]. In such a scattering process, an incident Cooper pair with spin  $\sigma$  mutually perpendicular to  $\mathbf{d}$  and  $\mathbf{M}$  acquires the spin- and orbital-dependent phase shift  $\pi - 2\sigma\phi + \Delta\theta$ : the first two terms are due to the spin flip, while the last is due to the phase change of the TSC gap upon specular reflection. Here  $\Delta\theta = \pi$  (0) for the  $p_x$  ( $p_y$ ) state, while  $\Delta\theta$  depends on the angle of incidence for the  $p_x + ip_y$  gap. It is well known that the gap is suppressed at interfaces where reflected Cooper pairs undergo a nontrivial phase shift [17]; in the TSC-FM junction we hence maximize the gap at the interface by choosing  $\phi$  so that the spin-flip reflected Cooper pairs have a  $2\pi n$  phase shift. Because of the different orbital phase shifts  $\Delta\theta$ , this occurs at  $\phi = 0$  ( $\pi/2$ ) for the  $p_x$  ( $p_y$ ) pairing amplitude, in agreement with Fig. 2. This interplay of spin and orbital degrees of freedom manifests an unconventional type of spin-orbital coupling at the TSC-FM interface.

*Stable moment orientation.*—The spin-spin and spin-orbital coupling effects give  $\phi$ -dependent contributions to the Gibbs free energy  $F$  of the junction, e.g., by modifying the local density of states in the FM and the condensation energy  $E_\Delta$  in the TSC, respectively. The energetically favored moment orientation is found directly

from  $F$ , while the relevance of the spin-orbital coupling can be deduced from  $E_\Delta$ . In Fig. 3 we present the behavior of the Gibbs energy  $F$  and the condensation energy  $E_\Delta$  as a function of  $\phi$ , where these quantities are evaluated for the pairing amplitudes that minimize  $F$  at the given angle [16].

In Fig. 3(a) we plot  $E_\Delta$  as a function of  $\phi$  for several typical cases and a perfect interface ( $t_{\text{int}} = 1$ ). As expected, the condensation energy for the  $p_x$  and  $p_y$  TSCs is indeed maximized for the exchange field orientation which maximizes the gap amplitude. The  $p_x + ip_y$  case is more complicated, since here the  $p_x$  and  $p_y$  gap components show opposite dependence upon  $\phi$ . We find that the maximum in  $E_\Delta$  shifts from  $\phi = \pi/2$  to  $\phi = 0$  with increasing exchange field strength. That is, for a weak FM the  $p_y$  component dominates the physics, while at strong polarizations the  $p_x$  gap is most important.

The minimum of the Gibbs free energy  $F$  fixes the stable moment orientation. In Figs. 3(b)–3(d), we plot  $F$  as a function of  $\phi$  for the three orbital symmetries at  $t_{\text{int}} = 1$ . For the  $p_x$  orbital symmetry, the profile exhibits a single minimum at  $\phi = 0$  and a maximum at  $\phi = \pi/2$ , and *vice versa* for the  $p_y$  TSC. The stable magnetic orientation is therefore parallel (perpendicular) to the  $\mathbf{d}$ -vector if the antinodes of the  $p$ -wave TSC gap are perpendicular (parallel) to the interface. Our conclusions are robust to changing  $t_{\text{int}}$  as shown in the Supplemental Material [16].

The Gibbs free energy for the  $p_x + ip_y$  junction has minima at both  $\phi = 0$  and  $\phi = \pi/2$ , which is not anticipated from the condensation energy. As shown in Fig. 3(d) and Fig. 4(a), at  $t_{\text{int}} = 1$  the global minimum shifts from  $\phi = \pi/2$  (perpendicular) to  $\phi = 0$  (parallel) with increasing exchange field strength. This occurs at the critical field strength  $h_{cr,1} \approx 1.74$ , which is a little higher than if we

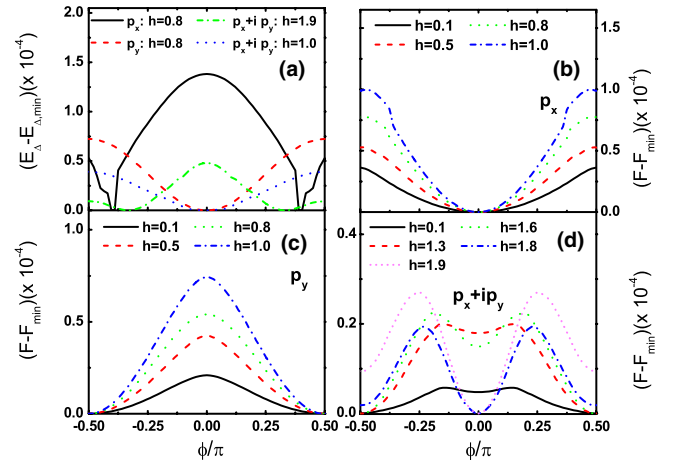


FIG. 3 (color online). (a) Dependence of the condensation energy  $E_\Delta$  on the angle  $\phi$ . (b)–(d) Dependence of the Gibbs energy  $F$  on  $\phi$  for various fixed  $h$  and for  $p_x$ ,  $p_y$ , and  $p_x + ip_y$  orbital symmetries of the TSC.  $E_{\Delta, \text{min}}$  and  $F_{\text{min}}$  are the minimum amplitudes of the related energies. All panels are for  $t_{\text{int}} = 1$  and temperature  $k_B T = 0.05$ .

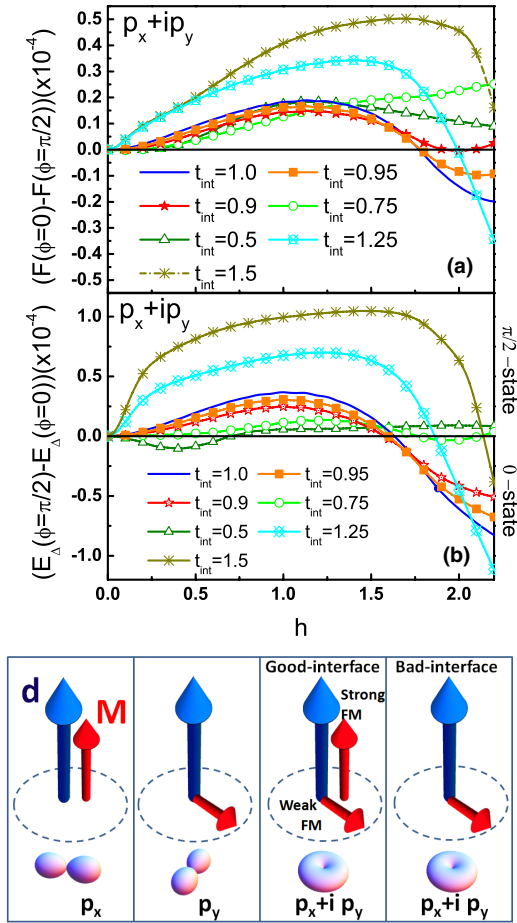


FIG. 4 (color online). (a) Gibbs and (b) condensation energy difference between the parallel ( $\phi = 0$ ) and perpendicular ( $\phi = \pi/2$ ) configurations of the moment as a function of the exchange field strength  $h$  and  $t_{\text{int}}$ , at temperature  $k_B T = 0.03$  for the  $p_x + ip_y$  TSC. Bottom panel: Sketch of the most favorable magnetic (small red arrow) configurations with respect to the orbital symmetry and the  $\mathbf{d}$ -vector (large blue arrow) of the TSC as well as the character of interface transparency.

considered only the condensation energy [see Fig. 4(b)]. Further increasing  $h$  into the extreme half-metal regime, we find that the  $\phi = \pi/2$  state reappears above  $h_{cr,2}$  (not shown). The two critical fields merge together as the temperature is increased, so that only the  $\phi = \pi/2$  state is stable sufficiently close to  $T_c$ . While the  $t_{\text{int}} > 1$  results are qualitatively similar, reducing  $t_{\text{int}}$  entirely suppresses the  $\phi = 0$  state. Here we also observe a decoupling between the condensation energy gain and the Gibbs free energy; e.g., for  $t_{\text{int}} \lesssim 0.8$  the gain in condensation energy in the low-field regime favors a  $\phi = 0$  state, while the Gibbs free energy shows that the  $\phi = \pi/2$  state is stable. Since the contribution to the free energy in the TSC region can be ascribed to  $E_{\Delta}$ , any inconsistency between the location of the minimum in  $F$  and  $E_{\Delta}$  must be due to the changes in the energy spectrum at the interface and in the FM, which are only included in the former. We expect that the modification

of the energy spectrum will depend rather strongly upon the interface hopping  $t_{\text{int}}$ , and indeed in Fig. 4 we observe that the condensation energy tends to overstate the stability of the  $\phi = 0$  state. We conclude that for a sufficiently imperfect interface the magnetization orientation is controlled by other processes, such as the change of the spectrum at the interface [11] or the proximity effect.

*Experimental considerations.*—The apparently small energy difference between the  $\phi = 0$  and  $\pi/2$  states shown in Fig. 4 results from averaging what is essentially an interface effect over the entire lattice; the energy gain per interface unit cell is  $L$  times larger, and gives an anisotropy energy on the order of  $\sim 0.01 k_B T_c$  for the microscopic parameters chosen here. In the case of a thin FM layer, the magnetic anisotropy induced by the coupling to the TSC could be observed by ferromagnetic resonance measurements: for an exchange field  $h = 0.5$  in the FM, and choosing  $\text{Sr}_2\text{RuO}_4$  ( $T_c = 1.5$  K) for the bulk TSC, we estimate a precession frequency of  $\sim 5 \cos(\phi)$  GHz. Since there is no spin-orbital coupling at SSC-FM interfaces, the observation of this precession would strongly indicate a TSC state in the superconductor. For a thicker layer, the TSC can modify the magnetization profile near the interface, effectively creating a spin-active boundary layer [18]. This may qualitatively alter the proximity effect and the electronic transport properties of the junction [7].

*Summary.*—In this Letter we have studied the interplay between orbital and spin degrees of freedom in a TSC-FM heterostructure. The orbital pairing state in the bulk TSC plays a critical role in fixing the stable orientation of the magnetization in the FM, which is summarized by the sketch in Fig. 4. For the time-reversal symmetric gaps, the easy axis in the FM originates from the maximization of the TSC's condensation energy. On the other hand, the orbital frustration of the condensation energy in a chiral TSC leads to a magnetic configuration with a first-order transition between the perpendicular and parallel configurations as a function of the exchange field. Spin-dependent electronic reconstruction at an imperfect interface can compensate the condensation energy gain. We argue that the induced anisotropy axis in the FM could be observed in ferromagnetic resonance measurements, and can act as a test of the orbital and spin pairing state of the TSC.

The authors thank M. Sigrist and C. Timm for useful discussions. This research was supported by the EU-FP7/2007-2013 under Grant Agreement No. 264098-MAMA.

- [1] D. Saint-James, D. Sarma, and E.J. Thomas, *Type II Superconductivity* (Pergamon, New York, 1969).
- [2] A.I. Buzdin, *Rev. Mod. Phys.* **77**, 935 (2005); F.S. Bergeret, A.F. Volkov, and K.B. Efetov, *ibid.* **77**, 1321 (2005).
- [3] V.V. Ryazanov, V. Oboznov, A. Rusanov, A. Veretennikov, A. Golubov, and J. Aarts, *Phys. Rev. Lett.* **86**, 2427 (2001).

- [4] F. S. Bergeret, A. F. Volkov, and K. B. Efetov, *Phys. Rev. B* **69**, 174504 (2004).
- [5] A. I. Buzdin and L. N. Bulaevskii, *Zh. Eksp. Teor. Fiz.* **94**, 256 (1988) [*Sov. Phys. JETP* **67**, 576 (1988)]; F. S. Bergeret, K. B. Efetov, and A. I. Larkin, *Phys. Rev. B* **62**, 11872 (2000).
- [6] M. Cuoco, A. Romano, C. Noce, and P. Gentile, *Phys. Rev. B* **78**, 054503 (2008).
- [7] M. Eschrig and T. Löfwander, *Nat. Phys.* **4**, 138 (2008); J. Linder, M. Cuoco, and A. Sudbø, *Phys. Rev. B* **81**, 174526 (2010).
- [8] G. Annunziata, M. Cuoco, C. Noce, A. Sudbø, and J. Linder, *Phys. Rev. B* **83**, 060508(R) (2011).
- [9] P. M. R. Brydon and D. Manske, *Phys. Rev. Lett.* **103**, 147001 (2009); B. Bujnowski, C. Timm, and P. M. R. Brydon, *J. Phys. Condens. Matter* **24**, 045701 (2012).
- [10] P. M. R. Brydon, *Phys. Rev. B* **80**, 224520 (2009).
- [11] P. M. R. Brydon, Y. Asano, and C. Timm, *Phys. Rev. B* **83**, 180504(R) (2011).
- [12] Y. Krockenberger, M. Uchida, K. S. Takahashi, M. Nakamura, M. Kawasaki, and Y. Tokura, *Appl. Phys. Lett.* **97**, 082502 (2010).
- [13] A. P. Mackenzie and Y. Maeno, *Rev. Mod. Phys.* **75**, 657 (2003).
- [14] Y. Oreg, G. Refael, and F. von Oppen, *Phys. Rev. Lett.* **105**, 177002 (2010); L. Jiang, D. Pekker, J. Alicea, G. Refael, Y. Oreg, and F. von Oppen, *ibid.* **107**, 236401 (2011).
- [15] K. Kuboki and H. Takahashi, *Phys. Rev. B* **70**, 214524 (2004).
- [16] See the Supplemental Material at <http://link.aps.org/supplemental/10.1103/PhysRevLett.111.097003> for details on the computational procedure.
- [17] L. J. Buchholtz and G. Zwicknagl, *Phys. Rev. B* **23**, 5788 (1981); C. Bruder, *ibid.* **41**, 4017 (1990).
- [18] D. Terrade, P. Gentile, M. Cuoco, and D. Manske, [arXiv:1210.5160](https://arxiv.org/abs/1210.5160) [*Phys. Rev. B* (to be published)].